



PRESSURE DISTRIBUTION IN A LAYERED RESERVOIR WITH GAS-CAP AND BOTTOM WATER

A.F. Owolabi^a, O.A. Olafuyi^b, E.S. Adewole^c

^aPETROLEUM ENGINEERING DEPARTMENT, UNIVERSITY OF BENIN, BENIN CITY, NIGERIA.
Emails: ^aalfaowoblow@yahoo.com; ^babdulkashif@yahoo.com; ^csteveadewole@yahoo.co.uk

Abstract

Oil production from a layered reservoir with a top gas cap and bottom water acting simultaneously poses serious challenges of rate and pressure maintenance. To achieve clean oil production both rates and pressures regimes have to be chosen carefully according to available to avert production of unwanted external fluids. Furthermore, well tests analyses of pressure data would require that flow from each layer is adequately quantified and delineated. For layers with crossflow interface isolating each layer through a test analysis is additional challenge. If the layers contain oil of different properties, well completion strategy has to be specially crafted to achieve optimal individual layer production performance. It is with a view to addressing these challenges that this study becomes absolutely necessary. In this study, dimensionless pressure and dimensionless pressure derivatives are derived for each layer of a two layered reservoir, both drained through one vertical wellbore. The difference in flow behavior of the different layers is normalized, for crossflow layers, through a dimensionless time frame. The normalization enabled the crossflow layer to be treated as one enlarged reservoir and was utilized to discriminate flow from layers, no matter the choice of well completion and disparity in layer fluid properties. Flow times considered is elaborate and ranged from very early to early and late time, large enough for at least one of the external boundaries to be felt in a test period. Because the external boundaries impose a steady state, the emergence of steady state is considered as end of flow of clean oil in our computations. The characteristic signatures of the log-log plot of dimensionless pressures and pressure derivatives for early time and late flow periods were then used to characterize the reservoir system. It is revealed that time for clean oil production is longer for larger and thicker layers for constant production rate history. Furthermore, a flattening and a collapse to zero trends are observed on dimensionless pressure and dimensionless pressure derivative plots, respectively, when the effects of the top and/or bottom boundaries are felt. When a permeable interface is felt, similar trends are observed but there is cessation shortly afterwards depending on the degree of interlayer crossflow. Furthermore, it was noticed that perforation location does not seriously affect well productivities, especially at early times. Finally, only fluid ratios is recommended as adequate to reveal which of the external fluids accidentally reaches the wellbore during oil production, since each of the external fluids is capable of manifesting steady-state behavior.

Keywords: pressure derivatives, interlayer cross flow, heterogeneity, reservoir characterization, pressure distribution, dimensionless pressure

1. Introduction

Oil production from a layered reservoir with a top gas cap and bottom water acting simultaneously poses serious challenges of rate and pressure monitoring. The occurrence of any of these external boundaries may be artificial or designed to augment oil production. Either way, to achieve clean oil production and sustain it would be a serious challenge for the reservoir

engineer. Additional challenge is posed if the reservoir is compartmentalized or layered and the separating interface is permeable, i.e., allows oil crossflow from layer to layer. In this case, if the layers have oil of different properties, oil from each layer may have to be produced separately. This is more difficult than producing oil from both layers through one layer, requiring completion only in one layer. As a

way of getting over these challenges, regional oil production critical rates and pressure requirements are strictly adhered to. The only reliable way of determining these critical rates and pressures is utilizing flow dimensionless pressures and dimensionless pressure derivatives to thoroughly understand movement of fluid through the entire reservoir system. Expressions obtained could be used to formulate a well test analyses procedures to further identify the characteristics of the individual layers. From whichever layer the fluid is produced and under any fluid drive the reservoir fluid is produced (water-flooding or an enhanced recovery scheme), detailed layer information enables us to understand (1) conditions for early breakthrough of one layers fluid and thus obtain maximum oil recovery from each layer, and (2) correct strategy for efficient well completion.

The main objective of this study is to study the effects of layering on pressure distribution of a two-layered reservoir under both water bottom and a gas cap drive mechanism using dimensionless pressure and their derivatives. This will assist both the well completion and reservoir engineers to make decisions for clean oil production from either each layer, or in combination, even under these extremely hostile external boundary conditions. The characteristic signatures of the log-log plot of dimensionless pressure and pressure derivative at early and late flow times will be used in analyzing responses in the layered heterogeneous system.

In the 1980's, substantial efforts [1-5] were made to interpret multi-layered systems quantitatively with the introduction of production logging tools that measure the bottom hole pressure and flow rate simultaneously. The model considered in this work is identical to that of Bourdet [4-6] except that the layered reservoir considered here has both a top gas cap and a bottom water drive.

2. Reservoir System and Mathematical Description

As shown in Fig.1, a two-layered reservoir, containing oil of small and constant compressibility in each layer, is chosen for this study. A vertical well is drilled through the layers and one particular layer or both layers may be completed for production, depending on fluid dynamics and interlayer degree of crossflow. The reservoir is overlain at the top by a constant pressure gas-cap and at the bottom by bottom water. A mathematical model for the dimensionless pressure and dimensionless pressure derivative, based on real time, are desired for the layers to achieve our objectives. Applying the principle of superposition for constant rate, the pressure distribution in each layer is written down in for each layer as follows considering the interface and at least one external boundary:

Layer 1:

$$P_{D1} = -\frac{1}{2}Ei\left(-\frac{1}{4t_D}\right) - \frac{A_1}{2}Ei\left(\frac{r_{D1}^2}{4t_D}\right) - \frac{A_2}{2}Ei\left(-\frac{r_{D1}^2}{4t_D}\right) \quad (1)$$

Layer 2:

$$P_{D1} = -\frac{1}{2}Ei\left(-\frac{1}{4\alpha t_D}\right) - \frac{B_1}{2}Ei\left(\frac{r_{D1}^2}{4\alpha t_D}\right) - \frac{B_2}{2}Ei\left(-\frac{r_{D1}^2}{4\alpha t_D}\right) \quad (2)$$

In order to emphasize the radial flow regime, the derivative is taken with respect to the logarithm of time as [4]

$$P_D = \frac{dP_D}{d \ln t_D} = t_D \frac{\partial P_D}{\partial t_D} \quad (3)$$

Therefore, dimensionless pressure derivative expressions for Eqs.1 and 2 are derived as:

$$P_{D1}^1 = \frac{1}{2} \left[e^{-\frac{1}{4t_D}} + A_1 e^{-\frac{r_{D1}^2}{4t_D}} + A_2 e^{-\frac{r_{D2}^2}{4t_D}} \right] \quad (4)$$

and

$$P_{D2}^1 = \frac{1}{2} \left[e^{-\frac{1}{4t_D}} + B_1 e^{-\frac{r_{D1}^2}{4t_D}} + B_2 e^{-\frac{r_{D2}^2}{4t_D}} \right] \quad (5)$$

3. Individual Layer and Boundary Characterization

While A_1 and B_1 are multiplicative factor for layers 1 and 2, respectively, A_2 and B_2 are constants characterizing the constant pressure external boundaries, i.e., the gas-cap and bottom water. To obtain expressions for the above constant, four boundary conditions come to play. At the interface, i.e., $z_D = f$,

$$P_{D1} = P_{D2}' \quad (6)$$

$$\frac{\partial P_{D1}}{\partial z_D} = M \frac{\partial P_{D2}}{\partial z_D} \quad (7)$$

At both ends of the z -axis, there is a constant-pressure condition at all times occasioned by a gas cap at the top and a bottom water at the bottom. Therefore, at the top of the reservoir, i.e., at $z_D = h_{De}$

$$\frac{\partial P_{D2}}{\partial t_D} = 0 \quad (8)$$

At the bottom of the reservoir, i.e., at $z_D = 0$

$$\frac{\partial P_{D1}}{\partial t_D} = 0 \quad (9)$$

Applying appropriate boundary conditions and solving, the following equations are obtained:

$$B_1 = -\frac{r_{D1}^2}{h_{De}^2} B_2 \exp -\frac{x_{D1}^2}{4\alpha t_D} \quad (10)$$

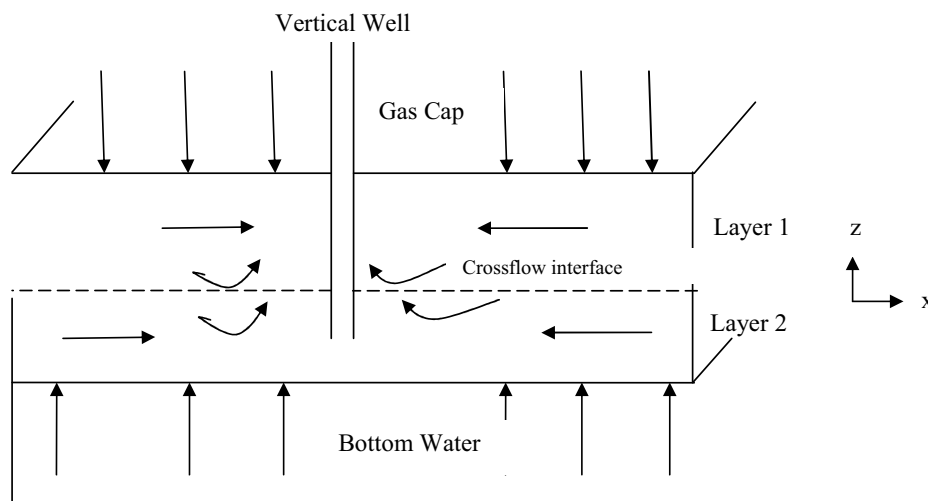


Figure 1: Reservoir and Well Model.

$$A_1 = -\frac{r_{D1}^2}{h_D^2} A_2 \exp -\frac{x_{D1}^2}{4t_D} \tag{11}$$

$$\frac{\left[E_i \left(-\frac{1}{4\alpha t_D} \right) - E_i \left(-\frac{1}{4t_D} \right) \right] \left[\frac{M f r^2 D_2}{(r_D h D_e)^2} \exp \left(-\frac{f^2}{4\alpha t_D} \right) - \frac{M}{f} \exp \left(-\frac{f^2}{4\alpha t_D} \right) \right]}{\frac{M f r^2 D_2}{(r_D h D_e)^2} \exp \left(-\frac{f^2}{4\alpha t_D} \right) - \frac{M}{f} \exp \left(-\frac{f^2}{4\alpha t_D} \right) - \exp \left(-\frac{f^2}{4t_D} \right) \left(\frac{1}{f} - \frac{f r_{D1}^2}{(h_D r_D)^2} \right)} \times \frac{1}{E_i \left(-\frac{f^2}{4t_D} \right) - \left(\frac{r_{D1}^2}{h_D^2} \exp \left(\frac{x_D^2}{4t_D} \right) E_i \left(-\frac{r_D^2}{4t_D} \right) \right)} \times \frac{r_{D2}^2 \exp \left(-\frac{x_D^2}{4t_D} \right) E_i \left(\frac{r_D^2}{4t_D} \right) E_i \left(-\frac{f^2}{4t_D} \right)}{1} = A_2 \tag{12}$$

$$\frac{\left[E_i \left(-\frac{1}{4\alpha t_D} \right) - E_i \left(-\frac{1}{4t_D} \right) \right] \left[\exp \left(-\frac{f^2}{4\alpha t_D} \right) \left(\frac{1}{f} - \frac{f^2 r_{D1}^2}{(h_D r_D)^2} \right) \right]}{\left[\frac{r_{D2}^2}{(h_{De})^2} \exp \left(\frac{x_D^2}{4t_D} \right) E_i \left(-\frac{r_D^2}{4t_D} \right) - E_i \left(-\frac{f^2}{4t_D} \right) \right] - \left[E_i \left(\frac{f^2}{4t_D} \right) - \left(-\frac{r_{D1}}{h_D^2} \exp \left(\frac{x_D^2}{4t_D} \right) \right) E_i \left(-\frac{r_D^2}{4t_D} \right) \right]} \times \frac{1}{\exp \left(-\frac{f^2}{4t_D} \right) - \left(\frac{1}{f} - \frac{f r_{D2}^2}{(h_D r_D)^2} \right)} \times \frac{1}{\frac{M f r_{D2}^2}{(r_D h D_e)^2} \exp \left(-\frac{f^2}{4\alpha t_D} \right) - \frac{M}{f} \exp \left(\frac{f^2}{4\alpha t_D} \right)} = B_2 \tag{13}$$

where $M = k_1 h_1 \mu_1 / k_2 h_2 \mu_2$, the interlayer fluid mobility ratio. In general,

$$r_D^2 = x_D^2 + f^2 \tag{14}$$

where f represents any dimensionless distance along the z -axis. From the definition of t_D ,

$$t_{D2} = \alpha t_{D1} \tag{15}$$

where α is a time normalization factor, specifying equivalent flow time in Layer 2 for a dimensionless flow t_D in L Layer 1, since the layers have different response times due to different in properties. It is the degree of interlayer crossflow. Detailed definitions of dimensionless parameters can be found in references [1-4].

4. Results and Discussion

Constant parameters used for computation are: $f = 0.25$, $x_D = 0.25$, $z_D = 0.7$, $\alpha = 10.0$, $M = 0.8$. These parameters were carefully selected to satisfy the physics governing flow in an undersaturated oil reservoir [3,5,7-8]. Dimensionless pressures were obtained by numerical computations using Matlab. Eq. 3 involves direct substitution to compute pressure derivatives.

4.1. Characterizing constants (A_1, A_2, B_1, B_2)

A plot of the four constants against time on semi-log axes is shown in Fig. 2.

It was noticed that at early time, the curves are not actually constant. Such times correspond to times

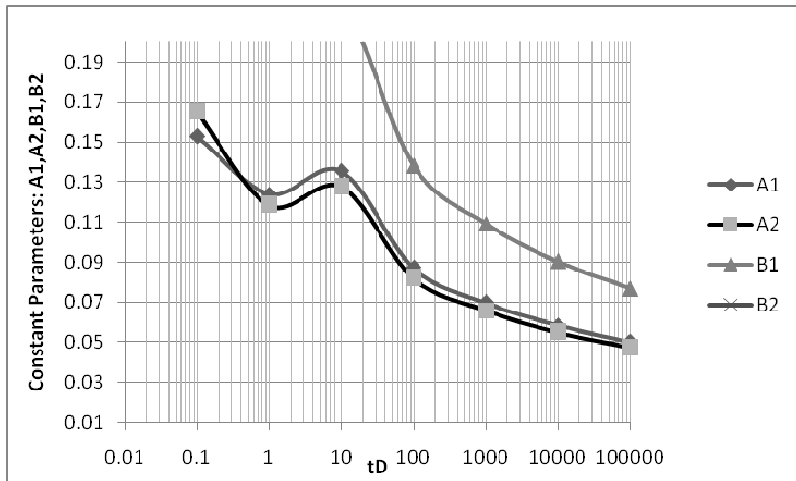
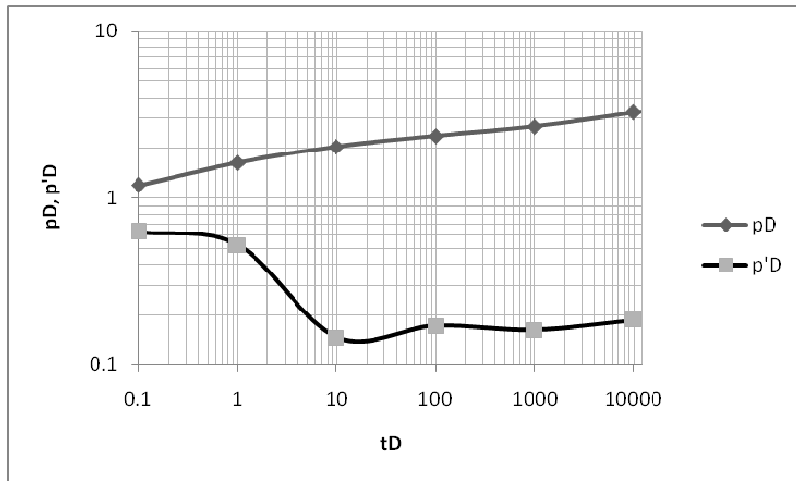
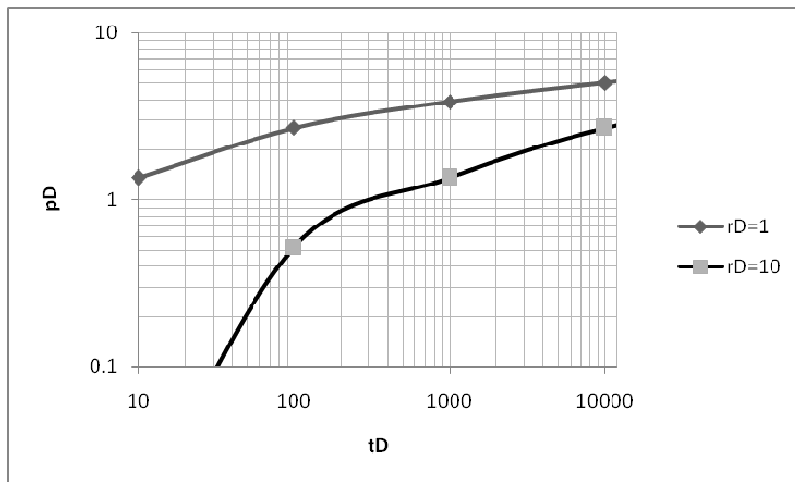


Figure 2: Plot of Constant Parameters on Semi-log Axes.



(a) Effects of layering on dimensionless pressure and pressure derivative for $x_D = 4.0$.



(b) Dimensionless pressures for different radial positions

Figure 3

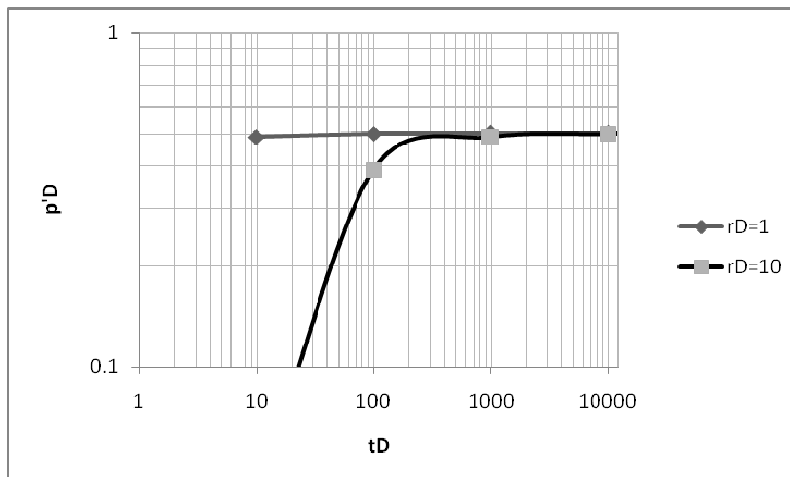


Figure 4: Dimensionless Pressure Derivative for Different Radial Positions.

when no boundary has been felt, hence, the results for the constants are trivial in the sense of application. At later times, when flow is far away from the wellbore, the parameters tend to be asymptotic with respect to the time axis irrespective of time. This time interval at which the constants maintain a zero slope marks the end of infinite-acting flow and attainment of their final values irrespective of flow time.

4.2. Effect of layering on pressure distribution

To study this effect, assume $f = 0.5$, $x_D = 4.0$, $z_D = 0.7$, $M = 0.9$, $\alpha = 10$. This means that the vertical well is completed in Layer 1 and oil production from the two layers takes place there. The value of $\alpha = 10$ and $M = 0.9$ means that for layers containing oil of the same viscosity and having the same thickness, the permeability of Layer 2 is higher than that of Layer 1 and the degree of crossflow of the interface is 10. Larger degree of crossflow would mean larger permeability of the interface. An interface with limited permeability would cause a long delay in interlayer flow.

On a log-log plot of dimensionless pressure versus dimensionless time shown in Fig 3, layering is the major cause of changes in gradients, especially at late flow dimensionless times. The different gradients indicate that different layers contribute to flow proportional to their local permeability. While it manifests in the pressure plot as gentle rise, in the derivative plot, it is seen as a depression. Since derivative plots are diagnostic plots to lend more meaning to dimensionless pressures, a depression on the derivative plot means that a constant-pressure boundary has been encountered and a rise subsequent to a depression means that another layer is contributing to flow. To identify which exact external boundary is contributing to flow, fluid ratios are utilized in the field. Increasing gas-oil

ratio would mean that the gas cap is contributing to flow, while an increasing water-oil ratio would mean that the bottom water is contributing to flow. Identification of actual external contributing to flow fluid is important in determining the best workover strategy to mitigate the production of unwanted fluid.

4.3. Validation of results

To validate our results, we now choose two arbitrary values of dimensionless radius, $r_D = 1$ and 10 and then compute dimensionless pressures and dimensionless pressure derivative over a period of dimensionless time. Results obtained, using Eq. 1 without the constants, denoting a vertical well producing oil from an infinite-acting reservoir are shown in Tables 1 and 2 and Figs 3 and 4.

From the above it is noticed that the pressure kept increasing monotonously with time. In Fig. 4, it is also noticed that the pressure derivative increased monotonously and stabilized at the inception of full radial flow to a value of 0.5 according to Ref. 4 to 5. Dimensionless wellbore radius 10 naturally takes a longer time to attain a derivative of 0.5 owing a larger sweep area than that of dimensionless radius of 1.

Having validated the results for an infinite-acting reservoir, we shall now proceed to obtain results considering the external boundaries to obtain pressure distribution for Layer 1, Layer 2 and extended reservoir to proffer useful interpretations.

4.4. Pressure distribution in Layer 1

The pressure distribution in Layer 1 was studied by considering completion of the well in Layer 1. This was achieved by simulating with $f = 0.5$, $x_D = 6.0$, $z_D = 0.7$, $M = 0.9$, $\alpha = 10$. For every value of $z_D > f$, the well simulated would be in Layer 1. The results in Table 5 were obtained:

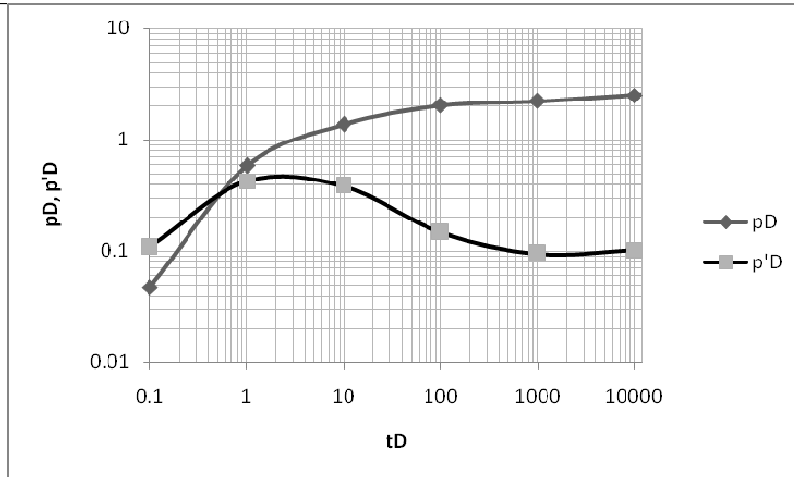


Figure 5: Log-log plot of dimensionless pressure and dimensionless pressure derivative for layer 1.

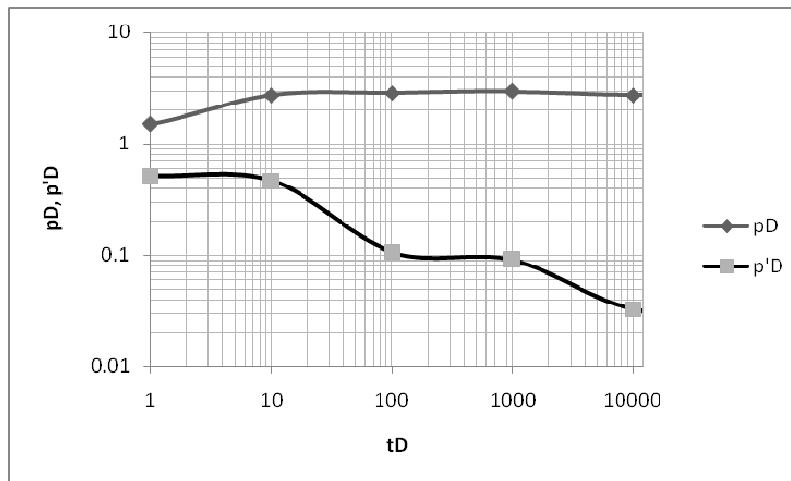


Figure 6: Log-log plot of dimensionless pressure and dimensionless pressure Derivative for layer 2.

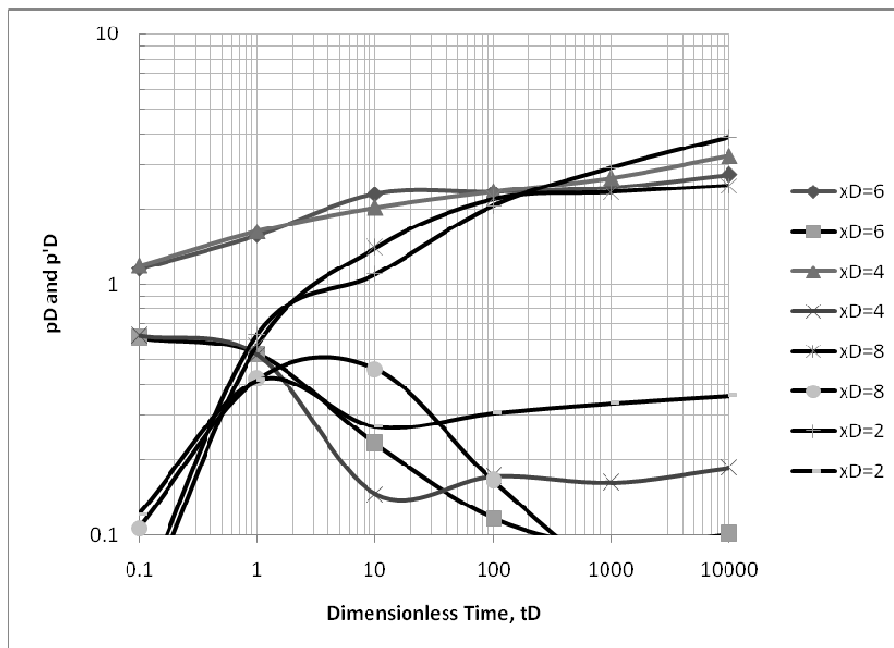


Figure 7: Dimensionless pressure and pressure derivative for several values of x_D .

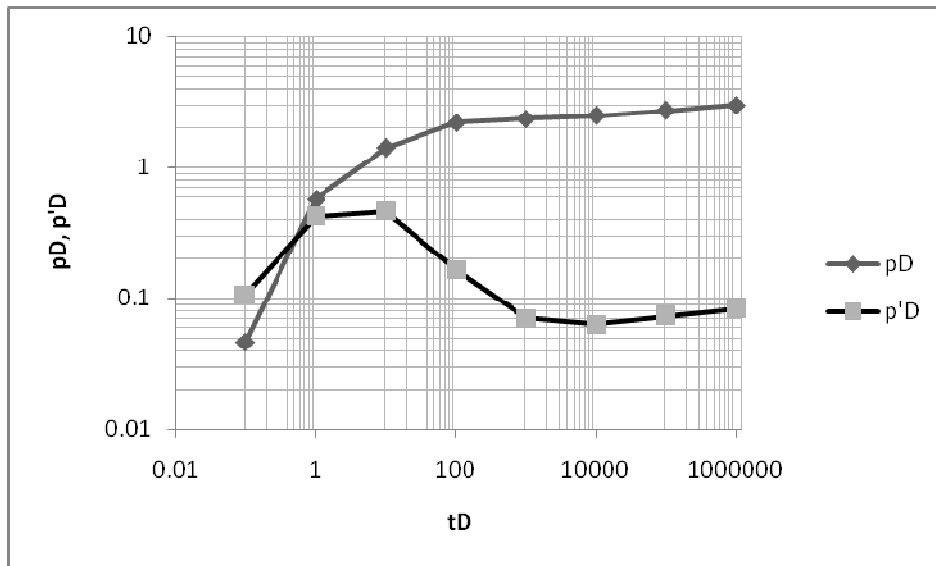


Figure 8: Dimensionless pressure and pressure derivative for $z_D = 0.8$.

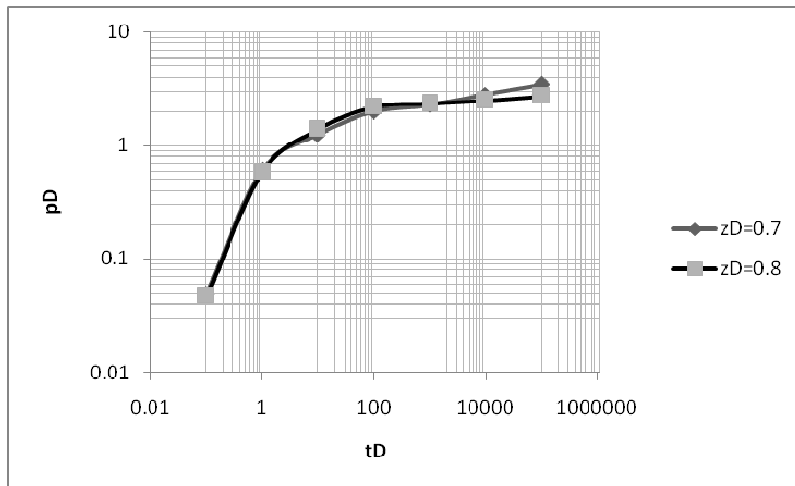


Figure 9: Dimensionless pressure for various positions of z_D .

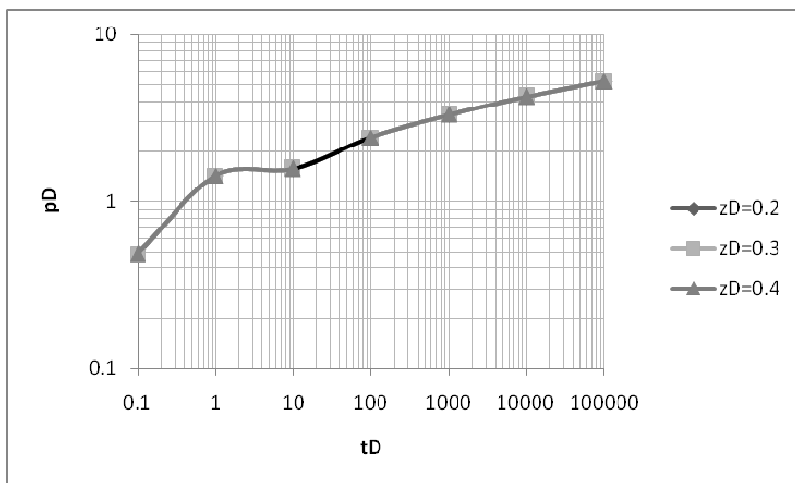


Figure 10: Dimensionless pressure for various positions of z_D .

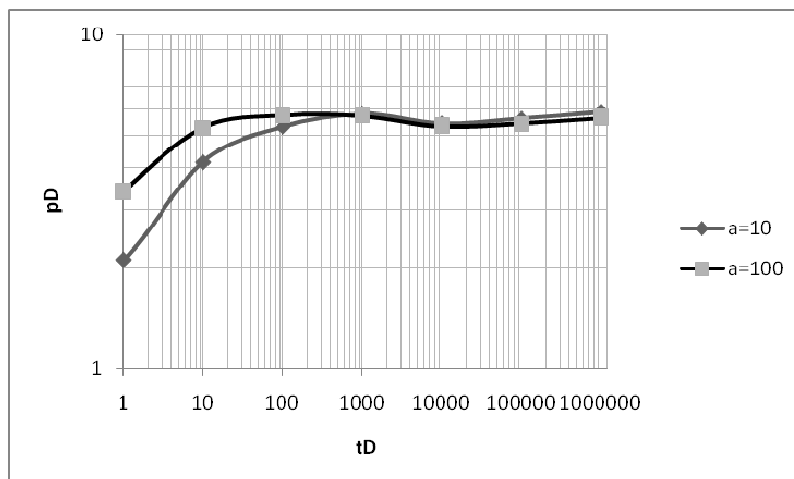


Figure 11: Dimensionless Pressure and Pressure Derivative for various values of α .

A plot of p_D and p'_D against t_D on a log-log scale is shown in the Fig. 5.

The trend exhibited by both dimensionless pressure and pressure derivative is very instructive. Looking closely at the pressure plot, it can be seen that between $t_D = 100$ and 10000 , the curve becomes flattened. This plateau-like surface on the curve indicates the influence of constant parameter $A1$ on the pressure transient generated. Within this time interval, a dampening effect is exhibited by Layer 1 leading to a reduction in the slope of the curve to zero. This is quite different from the standard plot where dimensionless pressure increases monotonously with time. At $t_D > 10000$, there is a gradual increase in the slope of the curve indicating that the transient has moved further away from the interface.

Furthermore, on the pressure derivative there is an initial increase to a maximum value of 0.5, after which there is a drastic decline at the same point where the inception of flattening in the pressure plot begins. This is agreeable with calculus since the derivative of a constant is approximately zero. Because of the constant pressure boundary, the derivative does not stabilize at 0.5 beyond end of infinite-acting period. The pressure derivative tends to drop gradually as the influence of the constant-pressure boundaries is felt. The rate of decline of the derivative response gives an indication of the sensitivity of the constant pressure boundaries to pressure drawdown at the wellbore. Similarly, the plot for Layer 2 is shown in Fig. 6, where the flattening is as a result of the bottom water.

4.5. Effect of flow parameters in 2-layered system

To further understand behaviour of the reservoir system and carefully identify parameters critical to

pressure distribution for the model, the effects of individual flow parameters were considered. x_D = lateral distance from the wellbore (along the x -axis).

4.6. Effects of lateral extent of the reservoir x_D

In order to expose the effect of the lateral distance from the wellbore, the value of x_D was varied while keeping other flow parameters constant as follows: $f = 0.5$, $x_D = 6.0$, $z_D = 0.3$, $M = 0.9$, $\alpha = 10$. The following results dimensionless pressures and their derivatives obtained are shown in Fig. 7 for extended reservoir conditions.

For both layers, the pressure plot becomes more flattened as the x_D increases. This implies that the effect of layering becomes more pronounced as the distance from the well bore increases in the x -direction. At smaller values of x_D , flow is very close to the wellbore and the pressure plot tends to conform with standard plots, behaving as if no external boundary is felt.

On the pressure derivative we noticed that it becomes steeper and the valley on the curve becomes deeper as x_D increases. This signifies more radial flow is possible the larger the lateral extent of the reservoir. Consequently, the effect of layering becomes more pronounced because of longer permeable interface.

It is therefore possible to achieve high degree of accuracy of analysis from conventional method if flow is very close to the wellbore. At such condition, the implicit assumption of a homogeneous system is valid making near wellbore characterization not only possible, but sufficiently accurate.

4.7. Effects of well position along the z -axis, z_D

Several well locations, z_D were chosen for our computation. Results obtained are shown in Figs. 8 to 10.

From the Figs. 8 and 9, it is evident that within a layer the variation of z_D has no effect on pressure distribution since the area under the curve for varying values of z_D remains constant. This is significant in the sense that it instructs the completion engineer to use the shortest pipe length to optimally drain from a given layer. The economic saving achieved here is worthwhile since there is reduction in the length of pipe required to penetrate more of the layer. In addition, it means that the well's productivity within a layer is independent of its position within that layer. However, productivity may differ from one layer to the other depending on the layer size and permeability.

4.8. Effects of degree of crossflow, α

Since the degree of cross-flow is an inter-layer parameter, to study its effect on pressure distribution, the total pressure distribution of the two layers was employed. Dimensionless pressures and their derivatives were computed for values of α for $f = 0.5$, $x_D = 6.0$, $M = 0.9$.

Results from Fig. 11, show that interlayer degree of communication does not affect flow performance of any layer at early flow times, if that layer is completed for production. Steady state occasioned by the top gas is experienced at the same time, irrespective of the value of α . However, the larger the α , the longer it takes for fluid in the other layer to respond to flow in one layer, but only in extended reservoir case. For all values of α larger than unity, well completion in Layer 2 would lead to early response of the layer to flow. This means quicker recovery from Layer 2.

5. Conclusion

For a two-layered reservoir with a top gas and bottom water, uninterrupted clean oil production is possible only with a deployment of correct well completion strategy gained from a good knowledge of the flow behaviour. Transient pressure responses of a two-layered reservoir system drained with a vertical well have been derived and factors affecting performance investigated. Results of the study show that:

1. Within one layer, the point at which the well is completed has no significant effect on the well's productivity.
2. Degree of crossflow affects only interlayer cross-flow; i.e., extended reservoir case.
3. Time for clean oil production is longer for larger and thicker layers for constant production rate.
4. A flattening and a collapse to zero trends are observed on dimensionless pressure and dimensionless pressure derivative plots, respectively, when the effects of the top and bottom boundaries are

felt. When a permeable interface is felt, similar trends are observed but there is cessation shortly afterwards depending on the degree of interlayer crossflow.

5. Oil production from separate layers is possible through a time frame dictated by commencement of interface effect.
6. Only fluid ratios can substantially establish external fluid produced in the wellbore, since a clear methodology is not derived for identifying any of the three constant boundaries that can felt under a given rate and pressure regime.

References

1. Earlougher, R.C., Kersch, K.M., and Kunzman, W.J. Some Characteristics of Pressure Buildup Behavior in Bounded Multiple-Layered Reservoirs Without Cross-flow. *Journal of Pet. Tech.*, Oct. 1974, Page 1178-1186.
2. Ehlig-Economides, C.A., and Joseph, J.A. *A New Test for Determination of Individual Layer Properties in a Multilayered Reservoir*. SPE Paper No. 14167, Presented at 1985 SPE Annual Technical Conference and Exhibition, Las Vegas, NV., Sept. 22-25.
3. Bennett, C.O., Reynolds, A.C., and Raghavan, R. Analysis of Finite Conductivity Fractures Intercepting Multilayer Reservoir. *SPE Formation Evaluation*, June, 1986, Page 259-274.
4. Bourdet, D. *Pressure Behavior of Layered Reservoirs with Crossflow*. SPE Paper No. 13628, presented at the 1985 Annual California Regional Meeting in Bakers, CA., Mar. 27-29.
5. Ehlig-Economides, C.A., and Joseph, J.A. *A New Test for Determination of Individual Layer Properties in a Multilayered Reservoir*. SPE paper No. 14167, presented at 1985 SPE Annual Technical Conference and Exhibition, Las Vegas, NV., Sept. 22-25.
6. Akhipemelo, D. and Adewole, E.S. Pressure Derivative Behavior of Two-Layered Reservoir with Vertical Wells. *Advanced Material Research*, vol. 1, 2008, Page 62-64.
7. Deans, H.A., and Gao, C-T. *Pressure Transients and Crossflow in a Multilayer Reservoir: Single-Phase Flow*. SPE Paper No. 11966, presented at the 1983 Annual Conference and Exhibition in San Francisco, CA., Oct. 5-8.
8. Earlougher, R.C., Kersch, K.M., and Kunzman, W.J. Some Characteristics of Pressure Buildup Behavior in Bounded Multiple-Layered Reservoirs Without Cross-flow. *J. Pet. Tech.*, Oct., 1974, 1178-1186.
9. Adewole, E.S. and Olafuyi, O.A. Comparison between Pressure Drop Profile of a Horizontal Well as a Water Injector and as an Oil Producer in a Five-Spot Waterflood Pattern. *Advance Material Research*, Vols. 18-19, 2007, Page 265-270.

Nomenclature

$A_1 = a_{11}$, $B_1 = b_{11}$, $A_2 = a_{12}$, $B_2 = b_{12}$: constant defining reservoir boundaries
 p_{D1} = dimensionless pressure for Layer 1
 p_{D2} = dimensionless pressure for Layer 2
 p'_{D1} = dimensionless pressure derivative for Layer 1
 p'_{D2} = dimensionless pressure derivative for Layer 2
 r_D = dimensionless radial distance from the wellbore
 x_D = dimensionless lateral distance from the wellbore along the x -axis
 z_D = dimensionless vertical distance along the z -axis
 $t_D = t_d$ = dimensionless time
 f = dimensionless interface well location
 M = mobility ratio, dimensionless
 α = interlayer flow normalization factor/degree of crossflow, dimensionless

10. Adewole E.S. and Olafuyi O.A. The Use of Source and Green's Functions to Derive Dimensionless Pressure and Dimensionless Pressure Derivative Distribution of a Two-Layered Reservoir (Part I: A-Shaped Architecture). *Journal of Mathematics and Technology*, Vol. 2. April Issue, 2010, Page 92-101.